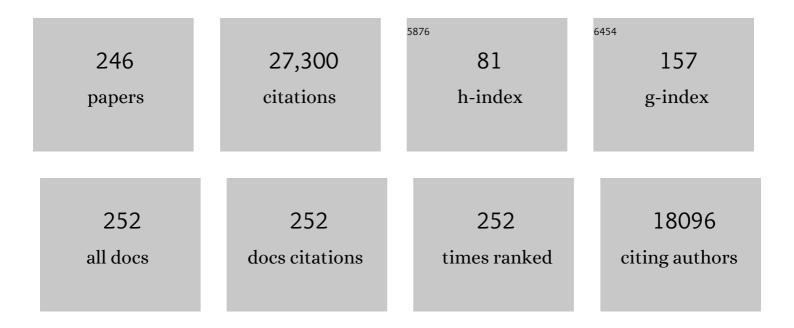
## **David Sinton**

List of Publications by Year in descending order

Source: https://exaly.com/author-pdf/8480826/publications.pdf Version: 2024-02-01



#	Article	IF	CITATIONS
1	CO <sub>2</sub> electroreduction to ethylene via hydroxide-mediated copper catalysis at an abrupt interface. Science, 2018, 360, 783-787.	6.0	1,638
2	Enhanced electrocatalytic CO2 reduction via field-induced reagent concentration. Nature, 2016, 537, 382-386.	13.7	1,429
3	CO <sub>2</sub> electrolysis to multicarbon products at activities greater than 1 A cm <sup>â~2</sup> . Science, 2020, 367, 661-666.	6.0	860
4	Dopant-induced electron localization drives CO2 reduction to C2 hydrocarbons. Nature Chemistry, 2018, 10, 974-980.	6.6	781
5	Electrochemical CO <sub>2</sub> Reduction into Chemical Feedstocks: From Mechanistic Electrocatalysis Models to System Design. Advanced Materials, 2019, 31, e1807166.	11.1	769
6	Molecular tuning of CO2-to-ethylene conversion. Nature, 2020, 577, 509-513.	13.7	682
7	Enhanced Nitrate-to-Ammonia Activity on Copper–Nickel Alloys via Tuning of Intermediate Adsorption. Journal of the American Chemical Society, 2020, 142, 5702-5708.	6.6	638
8	CO <sub>2</sub> electrolysis to multicarbon products in strong acid. Science, 2021, 372, 1074-1078.	6.0	541
9	Steering post-C–C coupling selectivity enables high efficiency electroreduction of carbon dioxide to multi-carbon alcohols. Nature Catalysis, 2018, 1, 421-428.	16.1	537
10	Microfluidic fuel cells: A review. Journal of Power Sources, 2009, 186, 353-369.	4.0	507
11	A New Generation of Sensors Based on Extraordinary Optical Transmission. Accounts of Chemical Research, 2008, 41, 1049-1057.	7.6	492
12	Multi-site electrocatalysts for hydrogen evolution in neutral media by destabilization of water molecules. Nature Energy, 2019, 4, 107-114.	19.8	470
13	Turning the Page: Advancing Paper-Based Microfluidics for Broad Diagnostic Application. Chemical Reviews, 2017, 117, 8447-8480.	23.0	439
14	Cooperative CO2-to-ethanol conversion via enriched intermediates at molecule–metal catalyst interfaces. Nature Catalysis, 2020, 3, 75-82.	16.1	390
15	Efficient electrically powered CO2-to-ethanol via suppression of deoxygenation. Nature Energy, 2020, 5, 478-486.	19.8	363
16	Copper nanocavities confine intermediates for efficient electrosynthesis of C3 alcohol fuels from carbon monoxide. Nature Catalysis, 2018, 1, 946-951.	16.1	354
17	Continuous Carbon Dioxide Electroreduction to Concentrated Multi-carbon Products Using a Membrane Electrode Assembly. Joule, 2019, 3, 2777-2791.	11.7	350
18	Binding Site Diversity Promotes CO <sub>2</sub> Electroreduction to Ethanol. Journal of the American Chemical Society, 2019, 141, 8584-8591.	6.6	338

#	Article	IF	CITATIONS
19	Metal–Organic Frameworks Mediate Cu Coordination for Selective CO <sub>2</sub> Electroreduction. Journal of the American Chemical Society, 2018, 140, 11378-11386.	6.6	326
20	Catalyst synthesis under CO2 electroreduction favours faceting and promotes renewable fuels electrosynthesis. Nature Catalysis, 2020, 3, 98-106.	16.1	325
21	A Microfluidic Fuel Cell with Flow-Through Porous Electrodes. Journal of the American Chemical Society, 2008, 130, 4000-4006.	6.6	301
22	Effect of compression on liquid water transport and microstructure of PEMFC gas diffusion layers. Journal of Power Sources, 2007, 163, 784-792.	4.0	281
23	Copper-on-nitride enhances the stable electrosynthesis of multi-carbon products from CO2. Nature Communications, 2018, 9, 3828.	5.8	279
24	Optofluidics for energy applications. Nature Photonics, 2011, 5, 583-590.	15.6	266
25	Nanoholes As Nanochannels: Flow-through Plasmonic Sensing. Analytical Chemistry, 2009, 81, 4308-4311.	3.2	264
26	Joule heating and heat transfer in poly(dimethylsiloxane) microfluidic systems. Lab on A Chip, 2003, 3, 141.	3.1	261
27	On-Chip Surface-Based Detection with Nanohole Arrays. Analytical Chemistry, 2007, 79, 4094-4100.	3.2	258
28	Magnetic Extraction of Microplastics from Environmental Samples. Environmental Science and Technology Letters, 2019, 6, 68-72.	3.9	242
29	High Rate, Selective, and Stable Electroreduction of CO <sub>2</sub> to CO in Basic and Neutral Media. ACS Energy Letters, 2018, 3, 2835-2840.	8.8	230
30	Constraining CO coverage on copper promotes high-efficiency ethylene electroproduction. Nature Catalysis, 2019, 2, 1124-1131.	16.1	214
31	Combined high alkalinity and pressurization enable efficient CO <sub>2</sub> electroreduction to CO. Energy and Environmental Science, 2018, 11, 2531-2539.	15.6	214
32	Designing anion exchange membranes for CO2 electrolysers. Nature Energy, 2021, 6, 339-348.	19.8	209
33	Hydroxide promotes carbon dioxide electroreduction to ethanol on copper via tuning of adsorbed hydrogen. Nature Communications, 2019, 10, 5814.	5.8	201
34	Photon management for augmented photosynthesis. Nature Communications, 2016, 7, 12699.	5.8	200
35	A Surface Reconstruction Route to High Productivity and Selectivity in CO <sub>2</sub> Electroreduction toward C <sub>2+</sub> Hydrocarbons. Advanced Materials, 2018, 30, e1804867.	11.1	200
36	2D Metal Oxyhalideâ€Derived Catalysts for Efficient CO <sub>2</sub> Electroreduction. Advanced Materials, 2018, 30, e1802858.	11.1	200

#	Article	IF	CITATIONS
37	High carbon utilization in CO2 reduction to multi-carbon products in acidic media. Nature Catalysis, 2022, 5, 564-570.	16.1	197
38	Chloride-mediated selective electrosynthesis of ethylene and propylene oxides at high current density. Science, 2020, 368, 1228-1233.	6.0	196
39	Efficient electrocatalytic conversion of carbon monoxide to propanol using fragmented copper. Nature Catalysis, 2019, 2, 251-258.	16.1	188
40	Improved fuel utilization in microfluidic fuel cells: A computational study. Journal of Power Sources, 2005, 143, 57-66.	4.0	162
41	Deep Learning with Microfluidics for Biotechnology. Trends in Biotechnology, 2019, 37, 310-324.	4.9	160
42	Self-Cleaning CO <sub>2</sub> Reduction Systems: Unsteady Electrochemical Forcing Enables Stability. ACS Energy Letters, 2021, 6, 809-815.	8.8	159
43	High-Density Nanosharp Microstructures Enable Efficient CO <sub>2</sub> Electroreduction. Nano Letters, 2016, 16, 7224-7228.	4.5	158
44	Cascade CO2 electroreduction enables efficient carbonate-free production of ethylene. Joule, 2021, 5, 706-719.	11.7	158
45	Electroosmotic flow with Joule heating effects. Lab on A Chip, 2004, 4, 230.	3.1	157
46	Single Pass CO <sub>2</sub> Conversion Exceeding 85% in the Electrosynthesis of Multicarbon Products via Local CO <sub>2</sub> Regeneration. ACS Energy Letters, 2021, 6, 2952-2959.	8.8	155
47	Efficient Methane Electrosynthesis Enabled by Tuning Local CO <sub>2</sub> Availability. Journal of the American Chemical Society, 2020, 142, 3525-3531.	6.6	154
48	Copper adparticle enabled selective electrosynthesis of n-propanol. Nature Communications, 2018, 9, 4614.	5.8	153
49	Pore-Scale Assessment of Nanoparticle-Stabilized CO <sub>2</sub> Foam for Enhanced Oil Recovery. Energy & Fuels, 2014, 28, 6221-6227.	2.5	150
50	Stable, active CO2 reduction to formate via redox-modulated stabilization of active sites. Nature Communications, 2021, 12, 5223.	5.8	145
51	Energy: the microfluidic frontier. Lab on A Chip, 2014, 14, 3127-3134.	3.1	144
52	Microfluidics for sperm analysis and selection. Nature Reviews Urology, 2017, 14, 707-730.	1.9	144
53	Hydronium-Induced Switching between CO <sub>2</sub> Electroreduction Pathways. Journal of the American Chemical Society, 2018, 140, 3833-3837.	6.6	144
54	Two-dimensional slither swimming of sperm within a micrometre of a surface. Nature Communications, 2015, 6, 8703.	5.8	135

#	Article	IF	CITATIONS
55	Nanomorphology-Enhanced Gas-Evolution Intensifies CO <sub>2</sub> Reduction Electrochemistry. ACS Sustainable Chemistry and Engineering, 2017, 5, 4031-4040.	3.2	135
56	Attomolar Protein Detection Using in-Hole Surface Plasmon Resonance. Journal of the American Chemical Society, 2009, 131, 436-437.	6.6	131
57	Rapid selection of sperm with high DNA integrity. Lab on A Chip, 2014, 14, 1142.	3.1	131
58	High-performance microfluidic vanadium redox fuel cell. Electrochimica Acta, 2007, 52, 4942-4946.	2.6	127
59	Efficient upgrading of CO to C3 fuel using asymmetric C-C coupling active sites. Nature Communications, 2019, 10, 5186.	5.8	127
60	Planar and three-dimensional microfluidic fuel cell architectures based on graphite rod electrodes. Journal of Power Sources, 2007, 168, 379-390.	4.0	123
61	Optofluidic Concentration: Plasmonic Nanostructure as Concentrator and Sensor. Nano Letters, 2012, 12, 1592-1596.	4.5	121
62	Chip-off-the-old-rock: the study of reservoir-relevant geological processes with real-rock micromodels. Lab on A Chip, 2014, 14, 4382-4390.	3.1	121
63	Direct DNA Analysis with Paper-Based Ion Concentration Polarization. Journal of the American Chemical Society, 2015, 137, 13913-13919.	6.6	121
64	Tuning OH binding energy enables selective electrochemical oxidation of ethylene to ethylene glycol. Nature Catalysis, 2020, 3, 14-22.	16.1	120
65	Hydrogen Peroxide as an Oxidant for Microfluidic Fuel Cells. Journal of the Electrochemical Society, 2007, 154, B1220.	1.3	115
66	Fluorescent Dyes for Visualizing Microplastic Particles and Fibers in Laboratory-Based Studies. Environmental Science and Technology Letters, 2019, 6, 334-340.	3.9	115
67	Oxygen-tolerant electroproduction of C <sub>2</sub> products from simulated flue gas. Energy and Environmental Science, 2020, 13, 554-561.	15.6	113
68	Aquifer-on-a-Chip: understanding pore-scale salt precipitation dynamics during CO2 sequestration. Lab on A Chip, 2013, 13, 2508.	3.1	112
69	An alkaline microfluidic fuel cell based on formate and hypochlorite bleach. Electrochimica Acta, 2008, 54, 698-705.	2.6	108
70	High-Rate and Efficient Ethylene Electrosynthesis Using a Catalyst/Promoter/Transport Layer. ACS Energy Letters, 2020, 5, 2811-2818.	8.8	106
71	Flow-Through vs Flow-Over: Analysis of Transport and Binding in Nanohole Array Plasmonic Biosensors. Analytical Chemistry, 2010, 82, 10015-10020.	3.2	103
72	Thermal end effects on electroosmotic flow in a capillary. International Journal of Heat and Mass Transfer, 2004, 47, 3145-3157.	2.5	101

#	Article	IF	CITATIONS
73	CO <sub>2</sub> Electroreduction to Formate at a Partial Current Density of 930 mA cm <sup>–2</sup> with InP Colloidal Quantum Dot Derived Catalysts. ACS Energy Letters, 2021, 6, 79-84.	8.8	100
74	Low coordination number copper catalysts for electrochemical CO2 methanation in a membrane electrode assembly. Nature Communications, 2021, 12, 2932.	5.8	97
75	Efficient electrosynthesis of n-propanol from carbon monoxide using a Ag–Ru–Cu catalyst. Nature Energy, 2022, 7, 170-176.	19.8	96
76	Flow-Directed Block Copolymer Micelle Morphologies via Microfluidic Self-Assembly. Journal of the American Chemical Society, 2011, 133, 18853-18864.	6.6	95
77	Carbon-efficient carbon dioxide electrolysers. Nature Sustainability, 2022, 5, 563-573.	11.5	95
78	Promoting CO2 methanation via ligand-stabilized metal oxide clusters as hydrogen-donating motifs. Nature Communications, 2020, 11, 6190.	5.8	93
79	Silica-copper catalyst interfaces enable carbon-carbon coupling towards ethylene electrosynthesis. Nature Communications, 2021, 12, 2808.	5.8	91
80	Lab-on-chip methodologies for the study of transport in porous media: energy applications. Lab on A Chip, 2008, 8, 689.	3.1	90
81	Suppressing the liquid product crossover in electrochemical CO <sub>2</sub> reduction. SmartMat, 2021, 2, 12-16.	6.4	90
82	Field-emission from quantum-dot-in-perovskite solids. Nature Communications, 2017, 8, 14757.	5.8	83
83	Microfluidic and nanofluidic phase behaviour characterization for industrial CO <sub>2</sub> , oil and gas. Lab on A Chip, 2017, 17, 2740-2759.	3.1	83
84	Rapid Microfluidics-Based Measurement of CO <sub>2</sub> Diffusivity in Bitumen. Energy & Fuels, 2011, 25, 4829-4835.	2.5	82
85	Steam-on-a-chip for oil recovery: the role of alkaline additives in steam assisted gravity drainage. Lab on A Chip, 2013, 13, 3832.	3.1	81
86	Bipolar membrane electrolyzers enable high single-pass CO2 electroreduction to multicarbon products. Nature Communications, 2022, 13, .	5.8	81
87	Nanohole arrays in metal films as optofluidic elements: progress and potential. Microfluidics and Nanofluidics, 2008, 4, 107-116.	1.0	79
88	Measurement of CO <sub>2</sub> Diffusivity for Carbon Sequestration: A Microfluidic Approach for Reservoir-Specific Analysis. Environmental Science & Technology, 2013, 47, 71-78.	4.6	79
89	Roadmap for optofluidics. Journal of Optics (United Kingdom), 2017, 19, 093003.	1.0	78
90	Full Characterization of CO <sub>2</sub> –Oil Properties On-Chip: Solubility, Diffusivity, Extraction Pressure, Miscibility, and Contact Angle. Analytical Chemistry, 2018, 90, 2461-2467.	3.2	78

#	Article	IF	CITATIONS
91	In Situ Formation of Nano Ni–Co Oxyhydroxide Enables Water Oxidation Electrocatalysts Durable at High Current Densities. Advanced Materials, 2021, 33, e2103812.	11.1	78
92	Electroosmotic velocity profiles in microchannels. Colloids and Surfaces A: Physicochemical and Engineering Aspects, 2003, 222, 273-283.	2.3	77
93	Emerging microalgae technology: a review. Sustainable Energy and Fuels, 2018, 2, 13-38.	2.5	74
94	Deep learning for the classification of human sperm. Computers in Biology and Medicine, 2019, 111, 103342.	3.9	73
95	Nanoporous Membranes Enable Concentration and Transport in Fully Wet Paper-Based Assays. Analytical Chemistry, 2014, 86, 8090-8097.	3.2	72
96	Enhanced multi-carbon alcohol electroproduction from CO via modulated hydrogen adsorption. Nature Communications, 2020, 11, 3685.	5.8	72
97	Gold-in-copper at low *CO coverage enables efficient electromethanation of CO2. Nature Communications, 2021, 12, 3387.	5.8	70
98	Fast Fluorescence-Based Microfluidic Method for Measuring Minimum Miscibility Pressure of CO <sub>2</sub> in Crude Oils. Analytical Chemistry, 2015, 87, 3160-3164.	3.2	68
99	Capillary Condensation in 8 nm Deep Channels. Journal of Physical Chemistry Letters, 2018, 9, 497-503.	2.1	65
100	Efficient electrocatalytic conversion of carbon dioxide in a low-resistance pressurized alkaline electrolyzer. Applied Energy, 2020, 261, 114305.	5.1	65
101	Bitumen–Toluene Mutual Diffusion Coefficients Using Microfluidics. Energy & Fuels, 2013, 27, 2042-2048.	2.5	64
102	Deep learning-based selection of human sperm with high DNA integrity. Communications Biology, 2019, 2, 250.	2.0	64
103	Morphological Control <i>via</i> Chemical and Shear Forces in Block Copolymer Self-Assembly in the Lab-on-Chip. ACS Nano, 2013, 7, 1424-1436.	7.3	61
104	Paper-Based Quantification of Male Fertility Potential. Clinical Chemistry, 2016, 62, 458-465.	1.5	60
105	Quantification of ovarian cancer markers with integrated microfluidic concentration gradient and imaging nanohole surface plasmon resonance. Analyst, The, 2013, 138, 1450.	1.7	58
106	Joint tuning of nanostructured Cu-oxide morphology and local electrolyte programs high-rate CO <sub>2</sub> reduction to C <sub>2</sub> H <sub>4</sub> . Green Chemistry, 2017, 19, 4023-4030.	4.6	58
107	Nanomodel visualization of fluid injections in tight formations. Nanoscale, 2018, 10, 21994-22002.	2.8	56
108	Identification of Microfibers in the Environment Using Multiple Lines of Evidence. Environmental Science & Technology, 2019, 53, 11877-11887.	4.6	54

#	Article	IF	CITATIONS
109	High-efficiency electrokinetic micromixing through symmetric sequential injection and expansion. Lab on A Chip, 2006, 6, 1033.	3.1	53
110	Downstream of the CO <sub>2</sub> Electrolyzer: Assessing the Energy Intensity of Product Separation. ACS Energy Letters, 2021, 6, 4405-4412.	8.8	53
111	Controlled Self-Assembly of Quantum Dots and Block Copolymers in a Microfluidic Device. Langmuir, 2008, 24, 637-643.	1.6	52
112	Pressure Drop in Rectangular Microchannels as Compared With Theory Based on Arbitrary Cross Section. Journal of Fluids Engineering, Transactions of the ASME, 2009, 131, .	0.8	52
113	Condensation in One-Dimensional Dead-End Nanochannels. ACS Nano, 2017, 11, 304-313.	7.3	52
114	Accessory-free quantitative smartphone imaging of colorimetric paper-based assays. Lab on A Chip, 2019, 19, 1991-1999.	3.1	52
115	Increased Temperature and Turbulence Alter the Effects of Leachates from Tire Particles on Fathead Minnow ( <i>Pimephales promelas</i> ). Environmental Science & Technology, 2020, 54, 1750-1759.	4.6	52
116	Direct and Indirect Electroosmotic Flow Velocity Measurements in Microchannels. Journal of Colloid and Interface Science, 2002, 254, 184-189.	5.0	51
117	A plate-frame flow-through microfluidic fuel cell stack. Journal of Power Sources, 2011, 196, 9481-9487.	4.0	51
118	Boride-derived oxygen-evolution catalysts. Nature Communications, 2021, 12, 6089.	5.8	51
119	A microchanneled solid electrolyte for carbon-efficient CO2 electrolysis. Joule, 2022, 6, 1333-1343.	11.7	51
120	A penalty on photosynthetic growth in fluctuating light. Scientific Reports, 2017, 7, 12513.	1.6	50
121	Formation and Shear-Induced Processing of Quantum Dot Colloidal Assemblies in a Multiphase Microfluidic Chip. Langmuir, 2008, 24, 10596-10603.	1.6	49
122	Controlled Self-Assembly of Quantum Dotâ^'Block Copolymer Colloids in Multiphase Microfluidic Reactors. Langmuir, 2010, 26, 716-723.	1.6	49
123	Surface-enhanced Raman scattering (SERS) optrodes for multiplexed on-chip sensing of nile blue A and oxazine 720. Lab on A Chip, 2012, 12, 1554.	3.1	49
124	Microfluidic Manufacturing of Polymeric Nanoparticles: Comparing Flow Control of Multiscale Structure in Single-Phase Staggered Herringbone and Two-Phase Reactors. Langmuir, 2016, 32, 12781-12789.	1.6	48
125	Bubble nucleation and growth in nanochannels. Physical Chemistry Chemical Physics, 2017, 19, 8223-8229.	1.3	48
126	Biological Responses to Climate Change and Nanoplastics Are Altered in Concert: Full-Factor Screening Reveals Effects of Multiple Stressors on Primary Producers. Environmental Science & Technology, 2020, 54, 2401-2410.	4.6	48

#	Article	IF	CITATIONS
127	Disposable silicon-glass microfluidic devices: precise, robust and cheap. Lab on A Chip, 2018, 18, 3872-3880.	3.1	47
128	Microfluidic pore-scale comparison of alcohol- and alkaline-based SAGD processes. Journal of Petroleum Science and Engineering, 2017, 154, 139-149.	2.1	46
129	A miniaturized high-voltage integrated power supply for portable microfluidic applications. Lab on A Chip, 2004, 4, 87.	3.1	45
130	Nanoscale Phase Measurement for the Shale Challenge: Multicomponent Fluids in Multiscale Volumes. Langmuir, 2018, 34, 9927-9935.	1.6	45
131	Determination of Dew Point Conditions for CO <sub>2</sub> with Impurities Using Microfluidics. Environmental Science & Technology, 2014, 48, 3567-3574.	4.6	44
132	Numerical simulation of microfluidic injection processes in crossing microchannels. Journal of Micromechanics and Microengineering, 2003, 13, 739-747.	1.5	43
133	Out-of-plane ion concentration polarization for scalable water desalination. Lab on A Chip, 2014, 14, 681-685.	3.1	43
134	Exploring Anomalous Fluid Behavior at the Nanoscale: Direct Visualization and Quantification via Nanofluidic Devices. Accounts of Chemical Research, 2020, 53, 347-357.	7.6	43
135	A sequential injection microfluidic mixing strategy. Microfluidics and Nanofluidics, 2005, 1, 319-327.	1.0	42
136	Turning the corner in fertility: high DNA integrity of boundary-following sperm. Lab on A Chip, 2016, 16, 2418-2422.	3.1	42
137	Low pressure supercritical CO2 extraction of astaxanthin from Haematococcus pluvialis demonstrated on a microfluidic chip. Bioresource Technology, 2018, 250, 481-485.	4.8	42
138	Predominance of sperm motion in corners. Scientific Reports, 2016, 6, 26669.	1.6	41
139	Asphaltene Deposition during Bitumen Extraction with Natural Gas Condensate and Naphtha. Energy & Fuels, 2018, 32, 1433-1439.	2.5	41
140	CO <sub>2</sub> Electroreduction to Methane at Production Rates Exceeding 100 mA/cm <sup>2</sup> . ACS Sustainable Chemistry and Engineering, 2020, 8, 14668-14673.	3.2	41
141	Direct Visualization of Evaporation in a Two-Dimensional Nanoporous Model for Unconventional Natural Gas. ACS Applied Nano Materials, 2018, 1, 1332-1338.	2.4	40
142	Redox-mediated electrosynthesis of ethylene oxide from CO2 and water. Nature Catalysis, 2022, 5, 185-192.	16.1	40
143	Flow-Directed Assembly of Block Copolymer Vesicles in the Lab-on-a-Chip. Langmuir, 2012, 28, 15756-15761.	1.6	39
144	Machine learning for sperm selection. Nature Reviews Urology, 2021, 18, 387-403.	1.9	39

#	Article	IF	CITATIONS
145	Visualization and numerical modelling of microfluidic on-chip injection processes. Journal of Colloid and Interface Science, 2003, 260, 431-439.	5.0	38
146	A dynamic loading method for controlling on-chip microfluidic sample injection. Journal of Colloid and Interface Science, 2003, 266, 448-456.	5.0	38
147	Reducing the crossover of carbonate and liquid products during carbon dioxide electroreduction. Cell Reports Physical Science, 2021, 2, 100522.	2.8	38
148	Hand-powered microfluidics: A membrane pump with a patient-to-chip syringe interface. Biomicrofluidics, 2012, 6, 44102.	1.2	37
149	Microfluidic assessment of swimming media for motility-based sperm selection. Biomicrofluidics, 2015, 9, 044113.	1.2	37
150	Electroosmotic flow steers neutral products and enables concentrated ethanol electroproduction from CO2. Joule, 2021, 5, 2742-2753.	11.7	37
151	Eliminating the need for anodic gas separation in CO2 electroreduction systems via liquid-to-liquid anodic upgrading. Nature Communications, 2022, 13, .	5.8	37
152	Integrated electrochemical velocimetry for microfluidic devices. Microfluidics and Nanofluidics, 2007, 3, 403-416.	1.0	36
153	Microalgae on display: a microfluidic pixel-based irradiance assay for photosynthetic growth. Lab on A Chip, 2015, 15, 3116-3124.	3.1	36
154	Glycerol Oxidation Pairs with Carbon Monoxide Reduction for Low-Voltage Generation of C <sub>2</sub> and C <sub>3</sub> Product Streams. ACS Energy Letters, 2021, 6, 3538-3544.	8.8	36
155	Slab waveguide photobioreactors for microalgae based biofuel production. Lab on A Chip, 2012, 12, 3740.	3.1	35
156	Pore-scale analysis of condensing solvent bitumen extraction. Fuel, 2017, 193, 284-293.	3.4	35
157	Pore-scale analysis of steam-solvent coinjection: azeotropic temperature, dilution and asphaltene deposition. Fuel, 2018, 220, 151-158.	3.4	34
158	Microfluidics-based measurement of solubility and diffusion coefficient of propane in bitumen. Fuel, 2017, 210, 23-31.	3.4	33
159	Visualization of fracturing fluid dynamics in a nanofluidic chip. Journal of Petroleum Science and Engineering, 2018, 165, 181-186.	2.1	33
160	Thermally induced velocity gradients in electroosmotic microchannel flows: the cooling influence of optical infrastructure. Experiments in Fluids, 2004, 37, 872-882.	1.1	32
161	Changes in mineral reactivity driven by pore fluid mobility in partially wetted porous media. Chemical Geology, 2017, 463, 1-11.	1.4	32
162	Self-adaptive Bioinspired Hummingbird-wing Stimulated Triboelectric Nanogenerators. Scientific Reports, 2017, 7, 17143.	1.6	32

#	Article	IF	CITATIONS
163	Light dilution via wavelength management for efficient highâ€density photobioreactors. Biotechnology and Bioengineering, 2017, 114, 1160-1169.	1.7	30
164	Natural gas vaporization in a nanoscale throat connected model of shale: multi-scale, multi-component and multi-phase. Lab on A Chip, 2019, 19, 272-280.	3.1	30
165	Microfluidic Synthesis of Photoresponsive Spool-Like Block Copolymer Nanoparticles: Flow-Directed Formation and Light-Triggered Dissociation. Chemistry of Materials, 2015, 27, 8094-8104.	3.2	29
166	FertDish: microfluidic sperm selection-in-a-dish for intracytoplasmic sperm injection. Lab on A Chip, 2021, 21, 775-783.	3.1	29
167	Field tested milliliter-scale blood filtration device for point-of-care applications. Biomicrofluidics, 2013, 7, 44111.	1.2	28
168	Flow-Directed Loading of Block Copolymer Micelles with Hydrophobic Probes in a Gas–Liquid Microreactor. Langmuir, 2013, 29, 8385-8394.	1.6	28
169	Biomass-to-biocrude on a chip via hydrothermal liquefaction of algae. Lab on A Chip, 2016, 16, 256-260.	3.1	27
170	When robotics met fluidics. Lab on A Chip, 2020, 20, 709-716.	3.1	27
171	Dopant-tuned stabilization of intermediates promotes electrosynthesis of valuable C3 products. Nature Communications, 2019, 10, 4807.	5.8	26
172	Partial wetting gas–liquid segmented flow microreactor. Lab on A Chip, 2010, 10, 1732.	3.1	25
173	Laminar Fully Developed Flow in Periodically Converging–Diverging Microtubes. Heat Transfer Engineering, 2010, 31, 628-634.	1.2	25
174	Direct Measurement of the Fluid Phase Diagram. Analytical Chemistry, 2016, 88, 6986-6989.	3.2	25
175	Hydrothermal disruption of algae cells for astaxanthin extraction. Green Chemistry, 2017, 19, 106-111.	4.6	25
176	Radial sample preconcentration. Lab on A Chip, 2011, 11, 1102.	3.1	24
177	Culturing photosynthetic bacteria through surface plasmon resonance. Applied Physics Letters, 2012, 101, .	1.5	24
178	Lab-in-a-pen: a diagnostics format familiar to patients for low-resource settings. Lab on A Chip, 2014, 14, 957.	3.1	24
179	Nanoplastic State and Fate in Aquatic Environments: Multiscale Modeling. Environmental Science & Technology, 2022, 56, 4017-4028.	4.6	24
180	Wavelength-selective plasmonics for enhanced cultivation of microalgae. Applied Physics Letters, 2015, 106, .	1.5	23

#	Article	IF	CITATIONS
181	Prediction of DNA Integrity from Morphological Parameters Using a Singleâ€Sperm DNA Fragmentation Index Assay. Advanced Science, 2019, 6, 1900712.	5.6	23
182	A photosynthetic-plasmonic-voltaic cell: Excitation of photosynthetic bacteria and current collection through a plasmonic substrate. Applied Physics Letters, 2014, 104, 043704.	1.5	22
183	Self-assembled nanoparticle-stabilized photocatalytic reactors. Nanoscale, 2016, 8, 2107-2115.	2.8	22
184	Direct visualization of fluid dynamics in sub-10 nm nanochannels. Nanoscale, 2017, 9, 9556-9561.	2.8	22
185	Bubble Point Pressures of Hydrocarbon Mixtures in Multiscale Volumes from Density Functional Theory. Langmuir, 2018, 34, 14058-14068.	1.6	22
186	Effects of Hydrogen Peroxide on Cyanobacterium <i>Microcystis aeruginosa</i> in the Presence of Nanoplastics. ACS ES&T Water, 2021, 1, 1596-1607.	2.3	22
187	Microbubble lensing-induced photobleaching (?-BLIP) with application to microflow visualization. Experiments in Fluids, 2003, 35, 178-187.	1.1	21
188	Laminated thin-film Teflon chips for petrochemical applications. Lab on A Chip, 2012, 12, 4236.	3.1	21
189	Evanescent photosynthesis: exciting cyanobacteria in a surface-confined light field. Physical Chemistry Chemical Physics, 2012, 14, 4817.	1.3	21
190	A combined method for pore-scale optical and thermal characterization of SAGD. Journal of Petroleum Science and Engineering, 2016, 146, 866-873.	2.1	21
191	Paper-based sperm DNA integrity analysis. Analytical Methods, 2016, 8, 6260-6264.	1.3	21
192	Screening High-Temperature Foams with Microfluidics for Thermal Recovery Processes. Energy & Fuels, 2021, 35, 7866-7873.	2.5	21
193	Hydrodynamic dispersion of neutral solutes in nanochannels: the effect of streaming potential. Microfluidics and Nanofluidics, 2007, 3, 723-728.	1.0	20
194	Two-dimensional planar swimming selects for high DNA integrity sperm. Lab on A Chip, 2019, 19, 2161-2167.	3.1	20
195	Fractal Flow Patterns in Hydrophobic Microfluidic Pore Networks: Experimental Modeling of Two-Phase Flow in Porous Electrodes. Journal of the Electrochemical Society, 2010, 157, B760.	1.3	19
196	Digestible Fluorescent Coatings for Cumulative Quantification of Microplastic Ingestion. Environmental Science and Technology Letters, 2018, 5, 62-67.	3.9	19
197	Live sperm trap microarray for high throughput imaging and analysis. Lab on A Chip, 2019, 19, 815-824.	3.1	19
198	Effects of liquid conductivity differences on multi-component sample injection, pumping and stacking in microfluidic chips. Lab on A Chip, 2003, 3, 173.	3.1	18

#	Article	IF	CITATIONS
199	Microfluidics Underground: A Micro-Core Method for Pore Scale Analysis of Supercritical CO2 Reactive Transport in Saline Aquifers. Journal of Fluids Engineering, Transactions of the ASME, 2013, 135, .	0.8	18
200	Detection of bubble and dew point using optical thin-film interference. Sensors and Actuators B: Chemical, 2015, 207, 640-649.	4.0	18
201	Gold Adparticles on Silver Combine Low Overpotential and High Selectivity in Electrochemical CO <sub>2</sub> Conversion. ACS Applied Energy Materials, 2021, 4, 7504-7512.	2.5	18
202	Microplastics shift impacts of climate change on a plant-microbe mutualism: Temperature, CO2, and tire wear particles. Environmental Research, 2022, 203, 111727.	3.7	18
203	Optothermal sample preconcentration and manipulation with temperature gradient focusing. Microfluidics and Nanofluidics, 2012, 12, 221-228.	1.0	16
204	Selection of high-quality sperm with thousands of parallel channels. Lab on A Chip, 2021, 21, 2464-2475.	3.1	15
205	Concentrated Ethanol Electrosynthesis from CO <sub>2</sub> via a Porous Hydrophobic Adlayer. ACS Applied Materials & Interfaces, 2022, 14, 4155-4162.	4.0	15
206	Nanoparticle Stablized CO2 in Water Foam for Mobility Control in Enhanced Oil Recovery via Microfluidic Method. , 2014, , .		14
207	Surface Plasmon Resonance for Crude Oil Characterization. Energy & amp; Fuels, 2015, 29, 3019-3023.	2.5	13
208	Breathable waveguides for combined light and CO2 delivery to microalgae. Bioresource Technology, 2016, 209, 391-396.	4.8	13
209	Fluorescence in sub-10 nm channels with an optical enhancement layer. Lab on A Chip, 2018, 18, 568-573.	3.1	13
210	Geometrical Effects on the Temperature Distribution in a Half-Space Due to a Moving Heat Source. Journal of Heat Transfer, 2011, 133, .	1.2	12
211	Evanescent cultivation of photosynthetic bacteria on thin waveguides. Journal of Micromechanics and Microengineering, 2014, 24, 045017.	1.5	12
212	The Full Pressure–Temperature Phase Envelope of a Mixture in 1000 Microfluidic Chambers. Angewandte Chemie - International Edition, 2017, 56, 13962-13967.	7.2	12
213	Microfluidics and Their Macro Applications for the Oil and Gas Industry. The Way Ahead, 2015, 11, 8-10.	0.2	10
214	Accelerating Fluid Development on a Chip for Renewable Energy. Energy & Fuels, 2020, 34, 11219-11226.	2.5	10
215	Evaluation of a Microencapsulated Phase Change Slurry for Subsurface Energy Recovery. Energy & Fuels, 2021, 35, 10293-10302.	2.5	10
216	Past, Present, and Future of Microfluidic Fluid Analysis in the Energy Industry. Energy & Fuels, 2022, 36, 8578-8590.	2.5	10

#	Article	IF	CITATIONS
217	Toxicity of nanoplastics to zooplankton is influenced by temperature, salinity, and natural particulate matter. Environmental Science: Nano, 2022, 9, 2678-2690.	2.2	10
218	Dual gradients of light intensity and nutrient concentration for full-factorial mapping of photosynthetic productivity. Lab on A Chip, 2016, 16, 2785-2790.	3.1	9
219	Periodic harvesting of microalgae from calcium alginate hydrogels for sustained highâ€density production. Biotechnology and Bioengineering, 2017, 114, 2023-2031.	1.7	9
220	Deformation of microdroplets in crude oil for rapid screening of enhanced oil recovery additives. Journal of Petroleum Science and Engineering, 2018, 165, 298-304.	2.1	9
221	A Platform for Highâ€Throughput Assessments of Environmental Multistressors. Advanced Science, 2018, 5, 1700677.	5.6	8
222	Advances in Microfluidic Fuel Cells. , 2009, , 99-139.		6
223	The Full Pressure–Temperature Phase Envelope of a Mixture in 1000 Microfluidic Chambers. Angewandte Chemie, 2017, 129, 14150-14155.	1.6	6
224	Development of plasmonic substrates for biosensing. Proceedings of SPIE, 2008, , .	0.8	5
225	Microfluidic and nanofluidic integration of plasmonic substrates for biosensing. Proceedings of SPIE, 2009, , .	0.8	4
226	Microfluidic liquid actuation through ground-directed electric discharge. Microfluidics and Nanofluidics, 2011, 11, 653-662.	1.0	4
227	Biaxial nanohole array sensing and optofluidic integration. , 2008, , .		3
228	How to select ICSI-viable sperm from the most challenging samples. Nature Reviews Urology, 2021, , .	1.9	3
229	Dynamic Microfluidic Photomasking. Journal of Microelectromechanical Systems, 2007, 16, 1145-1151.	1.7	2
230	Portable audio electronics for impedance-based measurements in microfluidics. Journal of Micromechanics and Microengineering, 2010, 20, 087001.	1.5	2
231	AbCellera's success is unprecedented: what have we learned?. Lab on A Chip, 2021, 21, 2330-2332.	3.1	2
232	Nanohole Arrays in Metal Films as Integrated Chemical Sensors and Biosensors. Springer Series on Chemical Sensors and Biosensors, 2010, , 155-179.	0.5	1
233	Frontispiz: The Full Pressure–Temperature Phase Envelope of a Mixture in 1000 Microfluidic Chambers. Angewandte Chemie, 2017, 129, .	1.6	1
234	Planar and Three-Dimensional Microfluidic Fuel Cell Architectures. , 2007, , 941.		0

#	Article	IF	CITATIONS
235	Nanohole Arrays as Optical and Fluidic Elements for Sensing. , 2008, , .		Ο
236	Nanoplasmonics as nanofluidics: transport and sensing in flowthrough nanohole arrays. , 2011, , .		0
237	Novel Approach in Algae Biofuel Production using Advanced Photonics. , 2012, , .		Ο
238	Optofluidics for Energy: Fuel and Electricity From Plasmonically-Excited Photosynthetic Bacteria. , 2013, , .		0
239	Frontispiece: The Full Pressure–Temperature Phase Envelope of a Mixture in 1000 Microfluidic Chambers. Angewandte Chemie - International Edition, 2017, 56, .	7.2	Ο
240	Three-Dimensional Electrokinetic Focusing in a Planar Microstructure. , 2005, , .		0
241	Plasmonics. , 2010, , 18-1-18-37.		0
242	Plasmonically Enhanced Biofilm Photobioreactors. , 2013, , .		0
243	Efficient Electroreduction of CO2 in an Ultra-Slim Pressurized Electrolyzer. ECS Meeting Abstracts, 2019, , .	0.0	0
244	Carbon Dioxide Electroreduction to Multi-Carbon Products Using a Large-Scale Membrane Electrode Assembly. ECS Meeting Abstracts, 2019, , .	0.0	0
245	Stable, High-Rate CO2 Electroreduction to Multi-Carbon Products in a Membrane Electrode Assembly System. ECS Meeting Abstracts, 2019, , .	0.0	Ο
246	(Digital Presentation) Assessing the Energy Intensity of Product Purification in CO <sub>2</sub> Electrolysis. ECS Meeting Abstracts, 2022, MA2022-01, 2445-2445.	0.0	0